IEEE TENCON '93 / Beijing

Diagnosis of Melanoma with Fractal Dimensions

Vincent Ng[1] and Andrew Coldman[2],
[1] Terry Fox Laboratory, British Columbia Cancer Agency,
[2] Biometry Section, British Columbia Cancer Agency,
Vancouver, British Columbia, Canada. V5Z 1L3

Abstract *In this paper, we have been focused on the use of fractal concept in measuring the fuzziness of a mole. The box-counting method was used initially with two variations: fixed grid method and dynamic grid method. With the inherit difficulties in box-counting such as integral values of box sizes, we later investigated the variation method and the correlation method. However, the above methods depended on the segmentation result which separated a mole from its surrounding skin. In order to overcome the problem, we had experimented with two different methods which manipulated the intensities around the border of a mole. The first one calculated the size of the intensity surface area at different scales and the second method used the average absolute intensity difference of pixel pairs to obtain normalized fractional feature vectors. The paper reports the different ways of calculating the fractal dimensions and compares their differentiation power in the use of diagnosis of melanoma images.*

1 Introduction

Malignant melanoma is the most common cancer in people less than 35 years of age and incident rates are increasing by approximately 5% per annum in many white populations, including British Columbia. In 1987, Cascinelli [1] looked into using the computer to analyze cutaneous melanoma images. Recently, an imaging project in Australia had developed a computing system to assist in the distinction of melanoma(abnormal moles) from normal moles [2].

Early in 1991 we mounted a pilot study to develop computer programs to be used for differentiating normal and abnormal moles. Photographs of moles were digitized through the assistance of the Vision Laboratory of the Computer Science Department in Simon Fraser University. The imaging software was developed in house with the use of the graphics library for Sun workstations. Twelve different scores were calculated with respect to the shape, intensity and regularity of a mole's image. Two feature scores among the twelve were found to be significant upon statistical univariate analysis. They were *circularity* and *fractal dimension 1*[3].

2 Fractal Dimension

There are four clinical criteria to diagnosis a mole, namely shape, size, colour and irregularity of the border [4]. It is the fourth criterion which has raised our interest in applying the fractal concept to provide a measure to discriminate normal and abnormal moles.

The fractal concept was developed by Mandelbrot [5] to explain the ruggedness of natural surfaces. There are three principle characteristics of a fractal object. It has a large degree of heterogeneousness, a self-similar structure over different scales, and does not have a well-defined scale for describing its characteristics.

For a given image of a mole, we suggest two approaches to apply the fractal concept to model the regularity of the border of the mole. After the segmentation process, an image is separated into a mole region and a skin region. The border of the mole region can be modeled as a fractal curve and hence we can derive its corresponding fractal dimension. The methods in Section 3 are based on this approach. The second approach attempted to improve the accuracy by utilizing the intensity information of pixels around the border of a mole. Intensities of pixels are considered as fractal intensity surfaces in order to reduce the effect of inaccurate segmentation during the calculation of fractal dimensions. Two methods using this approach are described in Section 4. In this paper, D is used to represent a *fractal dimension* and H is the *Hurst coefficient*.

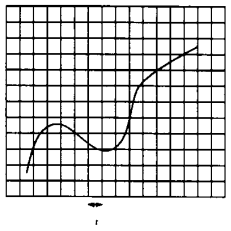

Figure 1: Fixed Grid Method

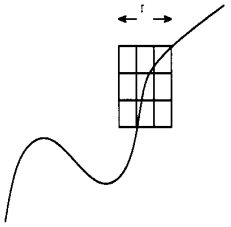

Figure 2: Dynamic Grid Method

3 Fractal Curves

The box counting method is one of the most popular techniques to estimate the fractal dimension of a set of points on a given curve L. The number of boxes, $N(r)$, of size r required to cover L has the following relationship [6]:

$$N(r) \propto \frac{1}{r^D}. \quad (1)$$

However, it is difficult to fit a minimum number of boxes covering L to obtain $N(r)$. An alternative method suggested in [6] is to divide the Euclidean space of the data points into grids of size $r \times r$ and count the number of boxes where L falls within. With this method, $N(r)$ becomes the number of boxes containing a piece of L.

FIXED GRID METHOD

We investigated two variations of the box counting method. The first method(C_1) divided an image into grids of pixels of size $r \times r$(see Figure 1). The number of grids which contain a piece of a mole's boundary in the image were counted as $N(r)$. Different values of r were used to obtain the corresponding $N(r)$'s. From equation (1), the fractal dimension, D, was obtained from the slope of the regression line of $log(r)$'s versus $log(N(r))$'s.

DYNAMIC GRID METHOD

The second method(C_2) obtained D by using many localized regions. The method moved a grid of pixels of size $r \times r$ along the border of the mole in an image. The center of the grid was always a boundary point of the mole. For each boundary point(P_i), the pixels within the grid and which lied on the border were counted(see Figure 2) to obtain $N_{P_i}(r)$. For each value of r, the counting process was repeated for all boundary points and the average value of $N_{P_i}(r)$'s was used as $N(r)$. Similar to C_1, the fractal dimension was obtained as the slope of the regression line of $log(N(r))$ versus $log(r)$.

VARIATION METHOD

The box counting methods depend on the covering of the fractal curve L with sequences of identical squares of size r. If r is close to a single pixel distance, the counts become unreliable. Furthermore, the size of an image will need to be divisble by r; otherwise some grids will extend beyond the image and it will falsify the counts and introduce irregularities to the least-square method. Our third method(C_3) was the variation method[7] which tried to reduce these problems by utilizing a geometric shape other than squares. If $f(x)$ is a continuous function representing L, we can define a horizontal segment $S(x, \eta)$ of length η with center at $(x, f(x))$. S is called the *horizontal structuring segment*. As S traverses L it sweeps an area A_η which is the union of all the $S(x, \eta)$(see Figure 3). The following equation from [7]

$$D = lim_{\eta \to 0}[2 - log(A_\eta)/log(\eta)] \quad (2)$$

shows that the rate of decrease of A_η as η decreases is directly related to the fractal dimension D. We had used different values of η's to find the corresponding A_η's for the border of a mole. The least-square method was used upon the logarithmic values of η and A_η and D equaled to the value of the resultant slope.

CORRELATION METHOD

The fourth method(C_4) was the correlation method [8]. It estimated the fractal dimension based on the statistics of pairwise distances. The *correlation integral*, $C(r)$, is a direct arithmetic average of the pointwise mass function for a set of points with distance r apart. The correlation dimension or the fractal dimension is defined in equation (3).

$$D = lim_{r \to 0} log(C(r))/log(r). \quad (3)$$

For a finite set of N data points, $C(r)$ can be approx-

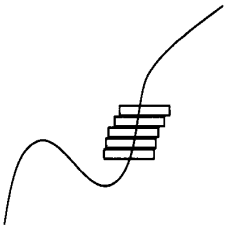

Figure 3: Variation Method

imated by $C(N,r)$ with the following equation[1]

$$C(N,r) = \frac{1}{N(N-1)} \sum_{i \neq j} \Theta(r - \| X_i - X_j \|) \quad (4)$$

where X_i and X_j are point i and point j respectively. This equation has the advantage that even when r is as small as the minimum interpoint distance, it maintains a good approximation for the correlation integral $C(r)$. The method was applied by moving a grid of size $r \times r$ along the border of the mole in an image.[2] The center of the grid was always a boundary point. At each boundary point, we used different values of r to obtain corresponding $C(N,r)$'s. The least-square method was used again for $log(C(N,r))$'s and $log(r)$'s. The resulting slope was the fractal dimension.

4 Fractal Intensity Surfaces

All the methods described in the previous section relied heavily on the segmentation result. For an abnormal mole, we would expected it to have a highly irregular border under which accurate segmentation of the image is difficult. If the border of a mole is not well-defined, the fractal concept can be used to model the unevenness of the pixel intensity surface.

INTENSITY SURFACE METHOD

The first intensity method(I_1) utilized the method described in [9]. The image intensity surface was modeled as a *fractal Brownian function* and was approximated by equation (5) in which the second-order statistics of the image changed with scale.

$$E(|\triangle I_{\triangle x}|) \; \|\triangle x\|^{-H} = E(|\triangle I_{\triangle x=1}|). \quad (5)$$

$E(|\triangle I_{\triangle x}|)$ was the expected value of the change in intensity over distance $\triangle x$. The method traced the contour of the mole region of an image with a grid of size $r \times r$. At each point P_i along the border, the grid was placed on top with P_i as the center. We calculated the quantities of $E(|\triangle I_{\triangle x}|)$ for different values of $\triangle x$ within the grid. The least squares method was used on the logarithmic values of the quantities and $\triangle x$'s to estimate H_{P_i}. The fractal dimension D_{P_i} at point P_i was equal to $2 - H_{P_i}$. The average of all the D_{P_i}'s along the border was reported.

FRACTAL FEATURE VECTOR METHOD

The previous method used the intensity surface area size as a function of scale. In the second intensity method(I_2), a normalized fractional Brownian motion feature vector[10] was used to represent the statistical features of the image surface from the fractional Brownian motion estimation concept. The method utilized the average absolute intensity difference of pixel pairs as a function of scale. For a grid of size $r \times r$, the normalized multiscale intensity difference vector (NMSID) consists of different absolute intensity difference averages for each reference scale. The k^{th} element of the vector is shown in equation (6) where $I(x_1,y_1)$ is the intensity value at point (x_1,y_1) and n_k is the total number of pixel pairs with distance $\triangle x$ and $k \leq \triangle x < k+1$.

$$NMSID_k = \sum_{x_1=0}^{r-1} \sum_{y_1=0}^{r-1} \sum_{x_2=0}^{r-1} \sum_{y_2=0}^{r-1} |I(x_2,y_2) - I(x_1,y_1)| / n_k. \quad (6)$$

With the NMSID's, the normalized fractional Brownian motion feature vector is $[f(1),...,f(k),...,f(n)]$ where $f(k) = log(NMSID_k) - log(NMSID_1)$ for k=1,2,...,n. In [10], Chen had shown that

$$f(k) = Hlog(\triangle x_k) - Hlog(\triangle x_1). \quad (7)$$

Therefore for an intensity surface of a mole's image, H was estimated by using the least-squares method on the values of $f(k)$'s and $log(k)$'s. We used the same technique as in I_1 to trace the border of a mole region and computed H_{P_i} at each boundary point. The fractal dimension, D_{P_i}, at P_i was equal to $3 - H_{P_i}$. The average values of all the D_{P_i}'s along the border was reported.

5 Results

14 photographs of moles were digitized into gray scale images of 256 levels. Seven of the 14 moles were abnormal moles. Each image had a pixel resolution of 512 x 512. All digitized images were transferred to a Sun SparcStation 2. Thresholding techniques were then applied to the images in order to segment them

[1] Θ is the Heaviside function: $\Theta(x)$ is zero for $x < 0$ and one for $x \geq 0$.

[2] Similar to the C_2 method.

	Mean (Normal)	Mean (Abnormal)	P-Value
C_1	1.104	1.337	0.064
C_2	1.126	1.196	0.654
C_3	1.194	1.271	0.084
C_4	1.323	1.433	0.084
I_1	1.372	1.411	0.655
I_2	1.806	1.729	0.084

Figure 4: Calculated Fractal Dimensions

	C_1	C_2	C_3	C_4	I_1	I_2
Seconds	2.3	2.4	3.5	77	2.7	2130.0

Figure 5: CPU Seconds Used in Calculating the Fractal Dimensions

according to their intensity distribution. Each image was transformed into a bi-level image which represented the two distinct regions. The darker region was the mole region and the brighter region was the skin region. A contour trace algorithm was applied to find out the border of the mole region.

After obtaining the boundary information, we processed all the 14 images to compute the fractal dimensions. Different values of r ranging from 5 to 17 were chosen for methods C_1, C_2, C_3 and C_4. The grid size for I_1 was 7 and the grid size for I_2 was 11. Each image had 6 different fractal dimensions calculated for the methods described in the previous sections. The Non-parametric Wilcoxon Rank Sum W test was used to compare the fractal dimensions between the normal and abnormal moles. The results are shown in Figure 4. The p-values indicate the difference of the distributions of fractal dimensions between the normal and abnormal moles of the methods. A method is good in differentiating the moles when it has a small p-value.

Amongst the methods, the box counting method with fixed grid(C_1) performed the best. It had a p-value of 0.064 and the difference between the means of normal and abnormal moles was ≥ 0.2. The variation method(C_3) performed as the second best. It had a p-value of 0.084 and a mean difference of 0.11. The correlation method(C_4) and fractal feature vector method(I_2) had similar performance. They both had a p-value of 0.084 and a mean difference of 0.077. In Figure 5, the average times required to calculate the fractal dimensions of the images are shown where C_1 was the most efficient method.

6 Conclusion

In this study, we applied the fractal concept in measuring the fuzziness of a mole. We had experimented with 6 different methods to obtain the fractal dimensions and found out the box counting method with fixed grid performed was the best in our images. Further work such as acquiring additional images of moles and researching for efficient computational algorithms will be investigated.

References

[1] N. Cascinelli, M. Ferrario, T. Tonelli, E. Leo. *A possible new tool for clinical diagnosis of Melanoma: The Computer*, Journal of the American Academy of Dermatology, Vol. 16(2/1) (Feb. 1987), pp. 361-367.

[2] A. Green, N. Martin, G. McKenzie, et al.. *Computer image analysis of pigmented skin lesions*, Melanoma Research, Vol. 1 (1991), pp. 231-236.

[3] V. Ng and A. Coldman. *Computerized Differentiation of Melanoma From Benign Pigmented Lesions*, Third Annual Western Canadian Society of Clinical and Investigative Dermatology Symposium, Feb. 20-23, 1992.

[4] V.T. DeVita, Jr., S. Hellman, and S.A. Rosenberg. *Cancer: Principles and Practice of Oncology*, Lippincott Company, 1985.

[5] B. B. Mandelbrot. *The Fractal Geometry of Nature*, San Francisco, CA:Freeman, 1982.

[6] Edited by H.O. Peitgen and D. Saupe. *The Science of Fractal Images*, Springer-Varlag, 1988.

[7] A. Le Mehaute. *Fractal Geometries: Theory and Applications*, CRC Press Inc., 1990.

[8] J. Theiler. *Estimating fractal dimension*, Optical Society of America, Vol. 7, No. 6 (June 1990), pp. 1055-1073.

[9] A.P. Pentland. *Fractal-Based Description of Natural Scenes*, IEEE Transactions on Pattern Analysis and Machine Intelligence, Vol. PAMI-6, No. 6 (Nov. 1984), pp. 661-674.

[10] C.C. Chen, J.S. Daponte and M.D. Fox. *Fractal Feature Analysis and Classification in Medical Imaging*, IEEE Transactions on Medical Imaging, Vol. 8, No. 2 (June 1989), pp. 133-141.